'91 KACC 1991. 10. 22~24

DETERMINING 3D-SHAPE OF SPECULAR OBJECTS BY USING AN ENCODED GRID PATTERN LIGHT SOURCE

Xiongying Ye and Sadao Fujimura

ORIX Computer System Co. University of Tokyo

Abstract

This paper describes a new method to determine the 3D-shape of objects consisting of specular planar surfaces. This method exploits a light source which is made of a diffuse plane with a grid pattern encoded in an M−sequence and uses a single image of the light source reflected by the objects to acquiring orientations and positions of the surfaces of the objects. When grid lines of the light source are reflected by a specular planar surface and perspectively projected on an image plane, a set of lines vanishing at a point are obtained on the image plane. The orientation of the specular planar surface is determined by using the vanishing point, and the position is determined by using the correspondence between lines on the image and lines on the light source, which is obtained by employing a characteristic regularity of the M−sequence. Before the vanishing points are calculated, the lines on the image are classified and correlated with the surfaces of objects by using slopes and positions of the lines and the regularity of the M−sequence. This method requires only a single image.

1 Introduction

This paper addresses the problem of determining three-dimensional shapes of specularly reflective objects. There is frequently a need to deal with specularly reflective objects such as metallic or glass objects in the manufacturing industries. However, most of the current methods to obtain 3D-shapes are based on an assumption that surfaces are diffusely reflective. Shape from shading[1] and photometric stereo[2] as well as slit lighting[3] and structured lighting techniques[4],[5] have used this assumption to reconstruct 3D-shapes from images.

Recently, some approaches to acquiring shapes of specular objects have been proposed. Koshikawa et al.[6] proposed a polarimetric method to obtain surface normals. In their method, they exploited the polarizational property of specular reflection which is a function of the incident angle and the refractive index of the material. Koshikawa's method can apply only to the objects whose refractive indices are constant. Ikeuchi[7] proposed a pseudophotometric stereo method, which determines surface orientations by using distributed light sources, images of reflected light sources and reflectance maps. Nishino et al.[8] developed Ikeuchi's method to determine the surface orientations and range information of specular polyhedrons. Ikeuchi's and Nishino's methods require a high degree of accuracy in brightness. Sanderson et al.[9] proposed a structured highlight approach that employs a scanned array of point sources and images of the resulting reflected highlights to compute local surface height and orientation. Sanderson' approach requires the use of many images because of scanning point sources.

In this paper we describe a new method for determining the 3D-shapes of objects consisting of specular planar surfaces. Our method exploits a diffuse plane light source with a grid pattern encoded in an M−sequence (maximum length sequence) and obtains orientations and positions of surfaces of objects from a single image.

2 Basic Relationships

In this section we derive the geometrical relationship between the parallel lines and their imaged lines which are obtained when the parallel lines are reflected by a specular planar and then perspectively projected on an image plane.

Parallel lines are reflected as parallel lines by a specular plane P. The specular plane is a bisecting plane of the original lines and the reflected lines. Thus, the normal vector $\vec{n}$ of the specular plane P is obtained by adding or subtracting the orientation vector $\vec{s}$ (unit vector) of original lines and the orientation vector $\vec{r}$ (unit vector) of reflected lines, that is,

$$\vec{n} = t(\vec{s} \pm \vec{r}), \tag{1}$$

where t is a proportional constant.

On the other hand, when parallel lines, $\{R_i\}$, as shown in Fig. 1, are perspectively projected onto an image plane, a set of lines $\{I_i\}$ converging at a point V are obtained on the image plane. This converging point V is called a vanishing point. The line which connects this vanishing point V and the projecting center O is parallel to the original parallel lines $\{R_i\}$, according to projective geometry. Thus, the orientation vector $\vec{r}$ of the original lines $\{R_i\}$ is represented as:

$$\vec{r} = (x_v - 0, y_v - 0, f - 0)/\sqrt{x_v^2 + y_v^2 + f^2}, \tag{2}$$

where x_v and y_v denote the coordinates of the vanishing point V on the image, and f is the focal length of the projection. The projecting center O is regarded as the origin (0,0,0).

Hence, the orientation of a specular planar surface can be determined by using known parallel source lines and projecting perspectively their reflected lines onto an image. In this case, the $\vec{r}$ of eq. (2) represents the orientation vector of the reflected lines and the normal vector of the

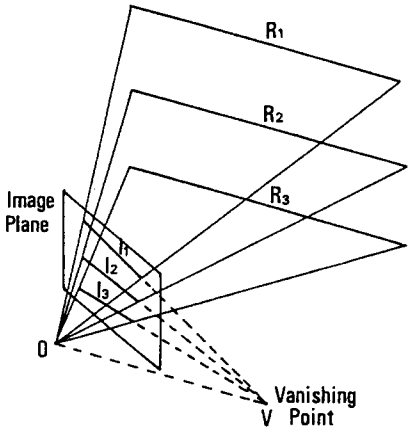

Figure 1: A vanishing point of a set of parallel lines.

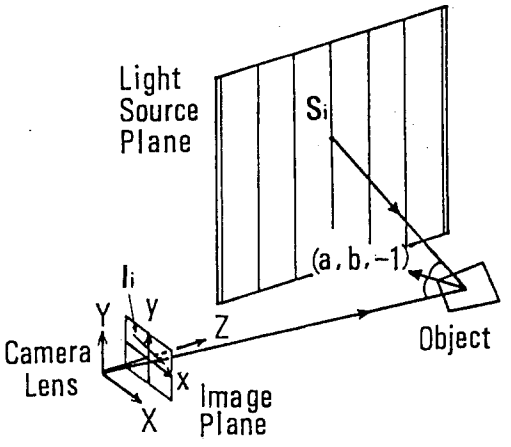

Figure 2: System configuration for determining 3D-shape of specular planar objects.

specular surface is obtained by substituting eq. (2) to the $\vec{r}$ of eq. (1).

2.1 Image of Reflected Source Lines

This method is structured according to the concept above. Figure 2 shows a system configuration. A diffuse plane light source with encoded parallel lines is exploited. Lines on the light source plane are reflected by a specular planar surface P and then perspectively projected onto the image plane through a camera lens O. From here on, a line on the light source plane will be referred to as a source line, and a line projected onto the image plane as an image line.

We derive the relationship between a source line and its corresponding image line. The origin of the world coordinate system is set at the center of the camera lens as shown in Fig. 2; and the optical axis of the camera is regarded as the Z-axis. The light source plane is set parallel to the YZ-plane and the source lines parallel to the Y-axis. The x- and y-axes of the image coordinate system are set parallel to the X- and Y-axes, respectively.

Let a planar surface P of interest be described by

$$Z = aX + bY + c. \tag{3}$$

A source line S_i parallel to the Y-axis is represented as

$$X = X_s \quad \text{and} \quad Z = Z_s. \tag{4}$$

When the source line S_i is reflected by a planar surface P and perspectively projected through the lens, an image line I_i is observed. Let the image line I_i be

$$\alpha x + \beta y + \gamma = 0, \tag{5}$$

and then α, β and γ satisfy the following equations:

$$\lambda\alpha = -2a(X_s + aZ_s) - 2c + Z_s(a^2 + b^2 + 1), \tag{6}$$

$$\lambda\beta = -2b(X_s + aZ_s), \tag{7}$$

$$\lambda\gamma = 2f(X_s + aZ_s) - 2acf - X_s f(a^2 + b^2 + 1), \tag{8}$$

where λ is a proportional constant [10].

2.2 Determination of the Parameters of a Planar Surface

The orientation parameters a and b of a specular planar surface P can be determined by eq. (1) when the orientation vector of the source lines $\vec{s}$ and that of the reflected lines $\vec{r}$ are known. In our system, $\vec{s}$ is

$$\vec{s} = (0, 1, 0) \tag{9}$$

and $\vec{r}$ is obtained from eq. (2) when the reflected lines are perspectively projected onto the image. Hence substituting eq. (2) and (9) into eq. (1), the normal vector $\vec{n} = (a, b, -1)$ of the planar surface P is obtained as

$$\begin{bmatrix} a \\ b \\ -1 \end{bmatrix} = t \begin{bmatrix} 0 \\ 1 \\ 0 \end{bmatrix} \pm \frac{t}{\sqrt{x_v^2 + y_v^2 + f^2}} \begin{bmatrix} x_v \\ y_v \\ f \end{bmatrix}. \tag{10}$$

By solving t from the 3rd row of eq. (10), and then by substituting t to the 1st and 2nd rows, a and b are obtained as

$$a = -\frac{x_v}{f}, \tag{11}$$

$$b = -\frac{1}{f}(y_v \pm \sqrt{x_v^2 + y_v^2 + f^2}). \tag{12}$$

The coordinates (x_v, y_v) of the vanishing point are determined by minimizing the sum of the square distances from the vanishing point V to image lines as

$$D^2 = \min \sum (\alpha_i x_v + \beta_i y_v + \gamma_i)^2, \tag{13}$$

where α_i, β_i and γ_i express α, β and γ of eq. (5) for each image line and it is satisfied that $\alpha_i^2 + \beta_i^2 = 1$.

Two values are obtained as b from eq. (12). However, we must determine a unique value of b for the planar surface P. This determination is done by acquiring the crossing line between the planar surface P and the light source

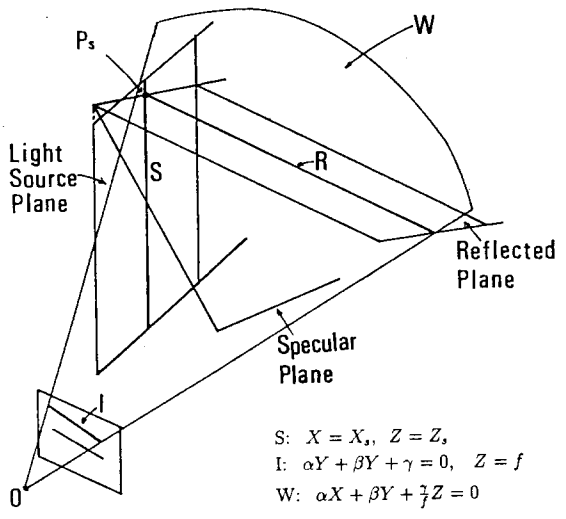

Figure 3: Illustration of a crossing point between a source line and the specular plane.

plane. A source line S and its reflected line R cross on the specular planar surface P (or its extension) at the point P_s as shown in Fig. 3. This crossing point P_s is also a crossing point of the source line S and the projecting plane W that includes the projecting center and the image line I corresponding to the source line S. Hence, the coordinates of P_s are obtained with the source line S and the projecting plane W [10] as

$$(X_s, -\frac{\alpha X_s + (\gamma/f) Z_s}{\beta}, Z_s).$$

Hence the crossing line between the planar surface P and the light source plane is determined from two or more crossing points such as the point P_s.

Let this crossing line on the light source plane ($X = X_s$) be

$$\frac{X - X_s}{0} = \frac{Y - Y_o}{q} = \frac{Z - Z_o}{1}. \tag{14}$$

The normal vector of the planar surface satisfies the followling equation

$$(0, q, 1) * (a, b, -1) = 0, \tag{15}$$

because this crossing line is on the planar surface P. Thus,

$$b = 1/q. \tag{16}$$

Therefore, the sign in eq. (12) is determined with the sign of q, and b is uniquely determined.

By eliminating λ in eq. (6) and eq. (7), the parameter c of the planar surface is expressed as

$$c = (\frac{\alpha}{\beta} b - a)(X_s + aZ_s) + \frac{Z_s(a_2 + b_2 + 1)}{2}. \tag{17}$$

We regard the mean value of c obtained from image lines and their respective source lines as the parameter c of the planar surface.

Thereby, all the parameters of the planar surface P are determined.

2.3 Determining Parameters of a Planar Surface Parallel to $Y-$axis

If a planar surface is nearly parallel to the Y-axis, i.e., $b \approx 0$, then the image lines from this planar surface are nearly parallel to the y-axis, i.e., $\beta \approx 0$. In this special case, the coordinates of the vanishing point and the crossing line between this planar surface and the light source plane are not calculated accurately. Consequently, we must determine the paramcters of such planar surfaces by another method. In this case, b^2 is ignored in eq. (6) and eq. (8), because it is known that $b^2 << a^2 + 1$. By eliminating λ in eq. (6) and eq. (8), the following equation results:

$$\frac{\gamma}{\alpha} \approx f \frac{2(X_s + aZ_s) - 2ac - X_s(a^2 + 1)}{-2a(X_s + aZ_s) - 2c + sZ_s(a^2 + 1)}. \tag{18}$$

And then, let

$$E = \sum (\gamma_i/\alpha_i - \widehat{\gamma_i/\alpha_i})^2, \tag{19}$$

where $\widehat{\gamma_i/\alpha_i}$ expresses the estimated value of γ_i/α_i for each image line. Parameters a and c are estimated by minimizing E with the Gauss-Newton iterative method, substituting eq. (18) into eq. (19) for each image line and its source line.

From eq. (6) and (7), b is obtained as follows:

$$b \approx \frac{\beta}{\alpha} \left(a + \frac{c}{X_s + aZ_s} - \frac{Z_s(a^2 + 1)}{2(X_s + aZ_s)} \right). \tag{20}$$

We use the mean value of b obtained from image lines and their respective source lines as the parameter b of the planar surface.

3 Application Problems

3.1 Encoded Pattern

In order to obtain surface parameters, matching image lines to source lines is necessary. We encode source lines with a period of an $M-$sequence in order to ease the matching. An $M-$sequence is the longest code sequence and is created by a primitive polynomial. The period of an $M-$sequence with order k equals $2^k - 1$. In a period of an $M-$sequence, any assortment except all zeros with k tuples appears once and only once. Thus, if k or more tuples are decoded, their position in a period is determined unambiguously. This is the reason we exploit an $M-$sequence to encode source lines. The encoding is accomplished by modifying brightness of the fringes between source lines. Figure 4 shows the brightness distribution of the light source pattern perpendicular to the fringes. The fine brightest fringes correspond to source lines. The

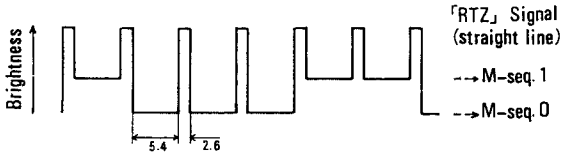

Figure 4: Brightness pattern of the light source encoded by $M-$sequence along Z-axis.

fringes with middle brightness correspond to the value 1 of the $M-$sequence, and the darkest fringes to the value 0 of the $M-$sequence.

3.2 Processing Algorithm

The algorithm to process images and reconstruct objects is given as follows:

1. Input an image.
2. Binarize the image to extract bright lines, and then thin the extracted bright lines.
3. Track the lines to find folding points. If there is a folding point on a line, then break this line at the folding point. If a line is shorter than the threshold, then eliminate the line.
4. Examine whether any two lines are considered as identical lines. If so, fill up the gap between them.
5. Fit an equation of straight line to points on a line for each line.
6. Classify and order lines according to their slopes and positions.
7. With respect to each class of lines, binarize the fringes between lines creating a binary sequence, and match the binary sequence to the $M-$sequence.
8. If there is an inconsistency on matching the $M-$sequence, then classify the lines again according to widths of the fringes between lines, and go to 7.
9. Compute parameters a, b, and c of planar surfaces with equations in section 2.2 or 2.3 depending on whether or not surfaces are parallel to the Y-axis.

In the case of the binarization to extract the bright lines, the image is decomposed into regions with 8x8 pixels and the threshold is determined as the mean of the maximum gray level and the average gray level for each region.

To fit an equation to a line, we assume the equation to be

$$x\cos\theta + y\sin\theta - \rho = 0 \qquad (21)$$

then determine θ and ρ by minimizing the sum of squared distances from points to the line. Here $\cos\theta$, $\sin\theta$ and $-\rho$ are α, β and γ of eq. (5), respectively.

We consider a surface with a class of lines on which the mean of values of (β/γ) is smaller than 0.07 [11] to be parallel to The Y-axis, and use equations of section 2.3 to compute its parameters.

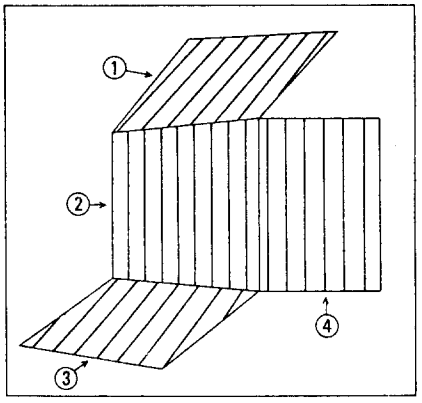

Figure 5: An example of image.

3.3 Classifying Lines

Since an object usually consists of several surfaces, we must classify lines to classes with each class corresponding to a surface. Consider an image as shown in Fig. 5. Assume that line set (1) and line set (3) belong on two planar surfaces with the same orientation, and line set (2) and line set (4) belong on two planar surfaces parallel to the Y-axis. First, a histogram of line slopes is used to classify lines because the slopes of lines on a surface approach each other. By this step, the lines on Fig. 5 can be classified to two classes: one includes line set (1) and line set (3), and the other line set (2) and line set (4). Second, histograms of center-point coordinates of lines are used to classify lines. By this step, line set (1) and line set (3) can be divided.

However, line set (2) and line set (4) cannot be segmented by the two above steps. The algorithm to segment these lines will be described in section 3.5.

3.4 $M-$sequence Matching

To match image lines to source lines, we first, binarize gray levels of fringes between lines and create a binary sequence $\{L_i | i = 1, \ldots, n\}$, where n is the number of fringes of a class. In the binarization, the mean of gray levels of pixels on a fringe is used as the fringe gray level, and the threshold is determined as the weighted mean of the maximum, minimum and the average gray levels of a class of fringes. From here on, we refer to the binary sequence as an image sequence.

Next, an image sequence is matched to the $M-$sequence $\{M_j | j = 1, \ldots, 2^k - 1\}$. The algorithm to match an image sequence to the $M-$sequence is shown as follows:

1. Match $L_1, \ldots, L_k$ to $\{M_j\}$ and let $j_0 = j$, where M_j corresponds to L_1.

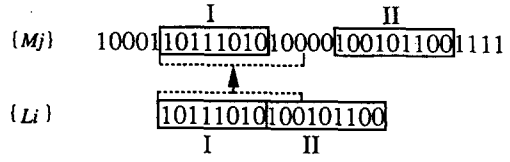

Figure 6: Matching an image sequence with two blocks to the $M-$sequence.

2. Let $i = k + 1$ and $j = j_0 + k$.

3. If $L_i \neq M_j$, go to segmentation (refer section 3.5).

4. Let $i = i + 1, j = j + 1$.

5. If $i > n$, end; or else go to 3.

If n is smaller than k, the image sequence cannot be uniquely matched to the $M-$sequence because of the character of the $M-$sequence. In this case, the orientation of the surface corresponding to this image sequence cannot be obtained uniquely, and the depth of this surface cannot be acquired.

3.5 Segmenting Lines

We use the inconsistency on matching the $M-$sequence and fringe widths in order to segment lines such as line set ② and line set ④ in Fig. 5.

The position of the boundary between line set ② and line set ④ can be determined roughly by matching the $M-$sequence. There is an inconsistency in the neighborhood of the boundary on matching the $M-$sequence, because line set ② and line set ④ are from unconnected places on the source plane, namely, from unconnected parts of the $M-$sequence.

However, the precise position of the boundary cannot be determined only by matching the $M-$sequence. This reason is demonstrated by Fig.6. Figure6 shows an example of the matching of an image sequence $\{L_i\}$, on which the block I and block II are created from the block I and block II of an $M-$sequence $\{M_j\}$ with the original polynomial $X^5 + X^2 + 1$. But the codebits of $\{L_i\}$ under the dashed line are matched to the codebits of $\{M_j\}$ with the dashed underline, on the matching. Consequently, the precise position of the boundary cannot be determined with the position of the inconsistency on matching the $M-$sequence.

To determine the precise position of the boundary, fringe widths are exploited. Fringe widths, that is, intervals between lines, are nearly equal on the same surface, while the width of the fringe at a boundary is usually different from others. Considering this fact, lines belonging to line set ② and to line set ④ can be divided by differentiating line intervals ($\Delta\rho$) in the neighborhood of the inconsistency on matching the $M-$sequence, and detecting the maximum.

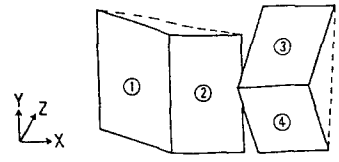

(a) Object to be measured

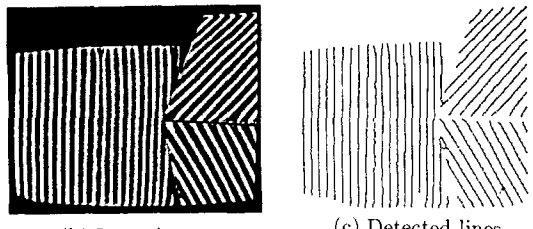

(b) Input image (c) Detected lines

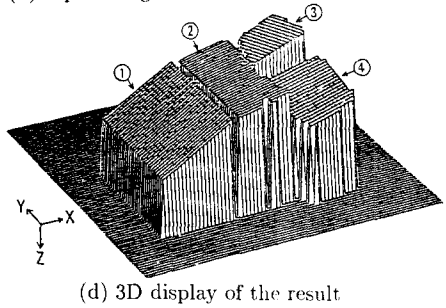

(d) 3D display of the result

Figure 7: An example of measurement

4 Experimental Results and Discussion

The experimental system is constructed as shown in Fig. 2. In this system, the light source plane whose size is 50 × 50cm^2 is placed parallel to the YZ-plane, at $X = -12$cm, between 15cm to 65cm along the Z-axis. The light source is an opal plate on which encoded lines are painted, and this opal plate is lighted from behind by three linear lamps arranged uniformly. There are 65 lines on the source plane. These source lines are encoded in an $M-$sequence period with the primitive polynomial $X^6 + X^4 + X^3 + X + 1$ ($k = 6$). Images are obtained by a CCD-camera with 256 × 240 pixels. The objects to be measured are placed in the range between 40cm and 70cm from the camera.

4.1 Results

We experiment with synthetic images and real images. The synthetic images are generated by the ray-tracing method. Table 1 shows estimated errors of results obtained with synthetic images. NP expresses surfaces not parallel to the Y-axis and PP surfaces parallel to the Y-axis. $\Delta\theta$ represents the orientation error between an estimated plane and its true plane, and ΔZ the error of depth. ΔZ is calculated as the average of absolute differences between Z-coordinates of boundary points on a estimated surface and that of points with the same (X, Y)

Table 1: Errors of surface normal and depth with synthetic images

Surface No.	NP1	NP2	NP3	NP4	NP5	NP6	NP7	NP8	PP1	PP2	PP3
$\Delta\theta^o$	0.15	0.09	0.72	0.15	0.67	0.08	0.22	0.98	0.06	0.05	0.26
ΔZ(mm)	1.1	0.1	2.4	0.2	3.6	0.2	0.9	6.5	0.14	0.86	1.02

on the true plane.

Figure 7 shows an example of the measurement of an object which consists of four stainless plates as shown in (a). (b) shows the input image, (c) the detected lines and (d) a 3D-display of the estimated results. In the results, four plates are all reconstructed, but surface ③ and surface ④ did not close because of the estimated errors. We also experimented with surfaces whose true parameters can be obtained. The estimated errors of results with these surfaces are shown in Table 2.

Table 2: Errors of surface normal with real images

Surface No.	NP1	NP2	PP3	PP4
$\Delta\theta^o$	5.9	1.3	0.6	2.5
ΔZ(mm)	23	1.2	2	15

4.2 Discussion

Considerable accuracy of estimation is obtained with synthetic images. However, estimated errors are slightly high with real images. The maximum error of orientation and depth is less than 1° and 7mm, respectively, with synthetic images, and 5.9° and 23mm, respectively, with real images. The errors of measuring true surfaces. estimating the camera parameters and setting the light source, increase estimated errors with real images. Moreover, when the bright lines extracted by binarizing are not complete, these lines can be curved by thinning. This can occur with real images and will increase estimated errors of results. In addition, with synthetic and real images, lines are curved by thinning when bright lines are cut slantingly by surface boundaries. This is also a reason for the decline in accuracy, especially in the case that detected lines are short. However, this decline can be overcome by improving the algorithm.

The surfaces which this system can measure are restricted to those whose orientation parameter a is from -2.2 to -0.2 and b from -1.9 to 1.9, because the size of the light source plane is limited. The size of a surface to be measured has to be so large that the surface can reflect $(k+1)$ lines to the image, because if the number of the lines corresponding to the surface is smaller than $(k+1)$, namely, the length of the corresponding image sequence smaller than k, then this image sequence cannot be uniquely matched to the $M-$sequence and the surface cannot be uniquely determined.

5 Conclusion

This paper described a new method to determine the 3D-shapes of objects which consist of specular planar surfaces by using a diffuse light source plane with an encoded grid pattern and an image.

This method needs only a single image. However, it cannot unambiguously determine the orientation and position of small surfaces. This is a subject for future study.

Acknowlendgment

The authors would like to express appreciation to Dr. N. Yamada of HP Co. for helpful advice and discussions. Thanks to Dr K. Kawakami Matsushita El. Ind. Co. for helpful advice.

References

[1] B. K. P. Horn, "Obtaining Shape from Shading Information," The Psychology of Computer Vision, P. H. Winston (ed.) McGraw-Hill, New York, 1975

[2] R. J. Woodham, "Photometric Stereo: A Reflectance Map Technique for Determining Surface Orientation from Image Intensity," Proc. SPIE 22nd Technical Symposium, Vol.155, San Diego, pp.136-143, 1978

[3] Y. Shirai, "Recognition of Polyhedra with Range Finder," Pattern Recognition, Vol.4, No.2, pp.243-250, 1972

[4] M. Minou, T. kanade and T. Sakai, "A Method of Time-coded Parallel Planes of Light for Depth Measurement," Trans. IECE Japan, Vol.E64, No.3, pp.521-528, 1981

[5] K. L. Boyer and A. C. Kak, "Color-Encoded Structured Light for Rapid Active Ranging," IEEE Trans. Pattern Anal. Machine Intell. Vol.PAMI-9, No.1, pp.14-28, 1987

[6] K. Koshikawa, "A Polarimetric Approach to Shape Understanding of Glossy Objects," Proc. 6th Int. Joint Conf. Artificial Intelligence, pp.493-495, 1979

[7] K. Ikeuchi, "Determining Surface Orientations of Specular Surfaces by Using the Photometric Stereo," IEEE Trans. Pattern Anal. Machine Intell., Vol.PAMI-3, No.6, pp.661-669, 1981

[8] E. Nishino and Y. Shirai, "Metal Surface Shape from Photometric Stereo Method with Light Projection," IPS Res. Rep. Japan, No.CV31-2, 1984

[9] A. C. Sanderson, L. E. Weiss and S. k. Nayar, "Structured Highlight Inspection of Specular Surfaces," IEEE Trans. Pattern Anal. Machine Intell., Vol.PAMI-10, No.1, pp.44-55, 1988

[10] X. Ye, "Study on Measurement of 3D-Shape Using M-sequence ded Grid," Ph.D. dissertation, Fac. Eng., Univ. Tokyo, in Japanese, 1989

[11] X. Ye, S. Fujimura and N. Yamada, "Determining 3D Shape of Glossy Objects by Using M-Sequence Encoded Grating Illumination" Trans. SICE Japan, Vol.26, No.2, pp.644-650, 1990